Research Square

Preprints are preliminary reports that have not undergone peer review.
They should not be considered conclusive, used to inform clinical practice,
or referenced by the media as validated information.

# Novel Oral-edaravone Attenuates Diastolic Dysfunction of Diabetic Cardiomyopathy via Activating the Nrf2 Signaling Pathway

**Ling Wang**
Kunming Medical University First Affilliated Hospital https://orcid.org/0000-0001-7451-6876
**Yue-Qin Zeng**
Kunming Medical University
**Juan-Hua Gu**
Kunming Medical University
**Rui Song**
Kunming Medical University Second Hospital
**Peng-Hui Cang**
Kunming Medical University
**Yong-Xuan Xu**
Kunming Medical University First Affilliated Hospital
**Xiao-xia Shao**
Kunming Medical University First Affilliated Hospital
**Li-Jin Pu** ( PLJ330@126.com )
Kunming Medical University First Affilliated Hospital https://orcid.org/0000-0002-2873-7210
**Hai-Yun Luo**
Kunming Medical University
**Xin-Fu Zhou**
University of South Australia

**Original investigation**

**Keywords:** novel oral-edaravone, diabetic cardiomyopathy, diastolic dysfunction, oxidative stress, Nrf2 signaling pathway

**Posted Date:** September 28th, 2021

**DOI:** https://doi.org/10.21203/rs.3.rs-936670/v1

**License:** This work is licensed under a Creative Commons Attribution 4.0 International License.
Read Full License

**Version of Record:** A version of this preprint was published at European Journal of Pharmacology on February 1st, 2022. See the published version at https://doi.org/10.1016/j.ejphar.2022.174846.

## Abstract

# Background

Diastolic dysfunction is the most common change of diabetic cardiomyopathy (DCM), but there is no effective clinical treatment at present. Oxidative stress plays a crucial role in the pathophysiological process of diabetic diastolic dysfunction including hypertrophy, apoptosis and fibrosis. The novel Oral-edaravone (OED) alleviates oxidative stress by scavenging free radical and may be suitable for the treatment of chronic diseases such as DCM.

# Methods

DCM was induced by high sugar and high fat diet with intraperitoneal injection of streptozotocin (STZ) in rats. OED (3mg/kg/day) was administration for 4 weeks. Cardiac structure and function were measured using transthoracic echocardiography. H9C2 cardiomyocytes with Nrf2 transfection or not were incubated in glucolipotoxicity and treated with OED for 48 hours to further explore the mechanism.

# Results

In type 2 diabetic rats,oral administration of OED for 4 weeks decreased malondialdehyde (MDA) and increased superoxide dismutase (SOD). OED significantly improved E/A ratio and myocardium hypertrophy accompanied by decreased cross-sectional area of cardiomyocytes, proportion of apoptotic cells, collagen volume fractions and depositions of collagen I/III. In H9C2 cells, OED reduced reactive oxygen species (ROS), cell surface area and TUNEL-positive cells induced by glucolipotoxicity. OED remarkably up-regulated the expression of the Nrf2 signaling pathway both in vivo and in vitro, further promoted Nrf2 nuclear translocation and up-regulated nicotinamide adenine dinucleotide phosphate quinone oxidoreductase (NQO1) and heme oxygenase (HO-1). Moreover, Nrf2 gene silencing abolished the protective effect of OED in H9c2 cells.

# Conclusion

Our findings demonstrated that OED treatment has the therapeutic potential to ameliorate diastolic dysfunction of DCM. The effect is mainly achieved by attenuating hyperglycemia and hyperlipidemia-induced cardiomyocytes hypertrophy, apoptosis and fibrosis via activating the Nrf2 signaling pathway.

## Background

The risk of heart failure in diabetes mellitus (DM) is increased more than twofold compared with individuals without DM,while diabetic cardiomyopathy (DCM) is the principal reason[1]. DCM has been proved to be independent on hypertension, coronary artery disease and valvular heart disease and

characterized by diastolic dysfunction[2], which is more common and earlier than systolic dysfunction[3]. The main pathological mechanisms of diabetic myocardial dysfunction are cardiomyocyte hypertrophy, apoptosis, collagen accumulation and interstitial fibrosis[4,5]. Myocardial remodeling induced by these pathophysiological changes is the main cause of diabetic myocardial diastolic dysfunction[6].

Oxidative stress injury is the main pathogenic factor of DCM[7,8]. Reactive oxygen species (ROS) is important to cell signaling and homeostasis, while inducing cell injury when dysregulated[9]. Overproduction of ROS caused by abnormal metabolism of diabetes, especially hyperglycemia and hyperlipidemia,is the main reason of oxidative stress inducing DCM[10]. Oxidative injury breaks the balance of physiological regulation in both cardiomyocyte and collagen synthesis, leading to cardiac hypertrophy, apoptosis and interstitial fibrosis[6]. Mitochondrial ROS production increases, oxidative phosphorylation is impaired and calcium is overloaded, leading to cell death[3,11]. Oxidative stress damage of endoplasmic reticulum can result in cell apoptosis by inducing protein misfold or degradation[12]. Previous studies have shown that antioxidant therapy is an effective measure in the treatment on DCM, more and more attention has been paid to the exploration of effective antioxidant drug and the potential mechanism[13,14].

Edaravone (ED) has potent free radical scavenging effects to alleviate oxidative stress. It has been applied to cerebral ischemia and reperfusion injury since 2001. Recent studies have shown that ED is effective on multiple target organs damage in diabetes. ED elevated superoxide dismutase, reduced malondialdehyde and increased corneal nerve fiber number in diabetic retinopathy[15,16]. In diabetes refractory wound healing, ED restored the repair capacity of the wound by scavenging ROS locally in the wound area[17]. It also exhibited direct protective effects against diabetic nephropathy by improving renal tubular cell function, reducing serum creatinine and renal vascular resistance[18]. Since DCM is a chronic disease, it is difficult to maintain effective and sufficient courses by treating patients with intravenous ED. The novel oral-edaravone (OED) obviously makes up for this deficiency. Jiao et al have confirmed that ED is also effective in Alzheimer'sdisease (AD) model[19] and Parikh et al generated a novel formula which showed efficacious in improving cognitive impairment in AD model[20,21]. However whether the OED is effective in DCM is not known. We propose that the chronic OED administration may be potential therapeutic agent for DCM. This study tests this hypothesis in the rat model of DCM.

Nuclear factor erythroid-derived 2 like 2 (Nrf2) is an important transcription factor in antioxidant response[22]. Researches revealed that the therapeutic effect of ED by alleviating oxidative stress in cerebral ischemia/reperfusion[23], neurologic impairment[24] and asthma[25] were achieved by activating the Nrf2 signaling pathway. Interestingly, Nrf2 is highly expressed in myocardial tissue[26] and protects myocardium from oxidative stress injury by regulating the expression of nicotinamide adenine dinucleotide phosphate quinone oxidoreductase (NQO1) and heme oxygenase (HO-1) and superoxide dismutase (SOD)[27]. Besides,the Nrf2 signaling pathway is closely associated with myocardial hypertrophy, apoptosis, fibrosis and dysfunction caused by oxidative stress injury[28]. We speculate that Nrf2 may be a key node at which OED exerts its effect to ameliorate diabetic cardiomyopathy. Therefore,

this study aims to elucidate the potential role and mechanism of OED in the prevention and treatment of DCM.

## Methods

# Animals model and experimental groups

Experiments were conducted according to the Guide for the care and Use of Laboratory Animal of National Institutes of Health (NIH Publication No.86 – 23, revised 1996) and approved by the Animal Research Ethics Committee of Kunming Medical University.

Eight-week-old male Sprague-Dawley rats, weighing 200-220g, were from the experimental animal center of Kunming Medical University. All rats, kept with 12h light/dark cycles at a constant temperature of 22 ± 3°C and more than 60% humidity, were fed adaptively for one week before experiment. The type 2 diabetic rat models were referred to the protocol reported in previous studies[29]. They were divided into three groups: normal control group (NC, n = 10), type 2 diabetes mellitus group (T2DM, n = 10) and OED-treated type 2 diabetes mellitus group (T2DM + OED, n = 10). OED was supplied from Suzhou Auzone Biotech (Fuzhou, Jiangsu). T2DM and T2DM + OED groups were fed on high glucose and high fat diet (comprising 52% standard chow diet, 18.5% protein, 10% fat, 15% saccharose, 3% egg powder, 1.5% cholesterol) and NC group was fed on standard chow diet in the entire process. All diets were obtained from the experimental animal center of Kunming Medical University. After 4 weeks, all rats were fasted for 12h before intraperitoneal injection to induce diabetes. Low dose STZ (35mg/kg,dissolved in 0.1M citrate buffer solution, PH 4.5) was injected in diabetic-induced rats and NC group was given equivalent volume of citrate buffer. Blood glucose and body weight were tested at day 1, 3, 7 and once a week for the rest of the experiment. Glucose levels consistently above 16.7mmol/L were enrolled. After STZ injection for one week, T2DM + EDA group was treated with OED (3mg/kg/d) by oral administration for four weeks. In the T2DM group, two rats died due to hyperglycemic hyperosmolar.

# Transthoracic echocardiography

Transthoracic echocardiography was performed to evaluate cardiac function of rat at experiment termination. All rats underwent transthoracic motion mode (M-mode), pulsed-wave Doppler (PWD) and two-dimensional echocardiography after anesthetized by 10% Chloral hydrate at a concentration of 0.3ml/100g. A blinded investigator used Philip EPIQ 7C machine equipped with a 3-12MHz surface probe to measure heart rates (HR), early diastolic peak velocity (E velocity), late diastolic peak velocity (A velocity), left ventricular internal dimension (LVIDd), left ventricular internal dimension in systole (LVIDs), interventricular septal thickness in diastole (IVSd), interventricular septal thickness in systole (IVSs), left ventricular posterior wall thickness at end diastole (LVPWd), left ventricular posterior wall thickness at end systole (LVPWs) and left atrial diameter (LAD) in two-dimensional and M-mode imaging. Besides, left ventricular ejection fraction (LVEF), left ventricular fractional shortening (LVFS), ratio of E and A velocity (E/A ratio), left ventricular mass (LVM) and ratio of left ventricular mass and body weight (LVW/BW) were calculated for analysis.

# Tissue samples

At the end of experiment, rats were anesthetized by intraperitoneal injection with pentobarbital (30 mg/kg). After phosphate buffered saline (PBS, Solarbio life sciences, Beijing, China) perfusion, all myocardial samples were quickly divided to liquid nitrogen and 4% paraformaldehyde for the next detection. For producing histopathological sections, the myocardial tissue were embedded in paraffin and cut to 5um. Protein was extracted using RIPA buffer (Beyotime Biotechnology, Shanghai, China) supplement with protease inhibitors (Roche Diagnostics GmbH, Mannheim, Germany). Isolation of myocardial cytoplasmic and nuclear components was performed according to the kit instructions (78833, Thermo Scientific, Massachusetts, US). Concentration of protein was determined by BCA assay kit (PC0020, Solarbio life sciences, Beijing, China).

# Enzyme linked immunosorbent assay (ELISA) analysis for Myocardial superoxide dismutase (SOD) and malondialdehyde (MDA)

The contents of SOD and MDA in tissue were determined according to the instructions of ELISA kits (JiangLai bio Ltd, shanghai, China.). SOD and MDA was expressed as ng/ml and nmol/ml individual.

# Hematoxylin and eosin (HE) staining and Masson staining

Paraffin embedded sections, sticking on glass slides, were stained with HE and Masson separately (Solarbio, Beijing, China). Five visualized fields of left ventricle sections were randomly captured with microscope (Leica, Germany) and Image Pro Plus6.0 software was used to calculate cardiomyocyte cross-sectional area and the area fraction of collagen.

# Immunohistochemistry

Myocardial tissue sections and primary antibody against collagen I (GB11022-3, Servicebio, Wuhan, China) and collagen III (GB13023-2, Servicebio, Wuhan, China) were incubated in 4°C refrigerator overnight. After washed with Phosphate Buffer Saline (PBS, Solarbio, Beijing, China) for three times, the second antibody was added and incubated at room temperature for 1 hour. Images were captured and data were analyzed using Image Pro Plus6.0.

# Terminal deoxynucleotidyl transferase-mediated dUTP nick end-labeling (TUNEL)

Cell apoptosis was detected by Terminal deoxynucleotidyl transferase-mediated dUTP nick-end labeling (TUNEL). According to the instructions of TUNEL kits (Roche Diagnostics GmbH, Mannheim, Germany; TUNEL BrightGreen Apoptosis Detection Kit, Vazyme, Nanjing, China), the slides were incubated with TUNEL reaction mixture at 37°C for 60 minutes. The apoptotic index was calculated as a percentage of positive apoptotic cells to the total cells.

# Cell culture and transfection

H9C2 cells were obtained from ATCC (CRL-1446, Manassas, US) and cultured in Dulbecco's modified Eagle's medium (DMEM, ATCC, Manassas, US) supplemented with 10% fetal bovine serum (FBS, Gibco, California, US) and 1% penicillin-streptomycin (Gibco, California, US), and maintained in a humidified incubator containing 5% CO2 at 37°C. Passages 2–8 of cells were used in the experiment. Transfection of cells was performed according to the manufacturer's instructions. H9c2 cells were transfected when reached 40% – 50% confluence. Nrf2 siRNA (sc-156128, Santa Cruz Biotechnology, US), control siRNA (sc-36869, Santa Cruz Biotechnology, US), and lipofectamine2000 (11668, Invitrogen, Thermo Scientific, Massachusetts, US) were diluted using opti-MEM (Gibco, California, US). Transfection was performed in medium without serum and antibiotic. After 7 hours, normal growth medium containing serum and antibiotics were added into plates and incubated the cells for an additional 24 h. The effect of gene silencing was confirmed using quantitative real-time polymerase chain reaction and western blotting. Cells were divided into five groups: normal group (NG, 25 mM glucose), high glucose and high fat group (HG/HF, 50mM glucose and 150uM sodium palmitate), and HG/HF with edaravone group (HG/HF + OED, 10ug/L edaravone), HG/HF + OED with Nrf2 siRNA group (HG/HF + OED + siNrf2) and HG/HF + OED with NC siRNA group (HG/HF + OED + siNC). After transfection, cells received OED (10ug/L) treatment for 48h in the condition of high glucose and high fat, except the normal group.

# Cell viability

Cell counting kit-8 (Lot.GB707, Dojindo Laboratories, Tokyo, Japan) was used to detect cell viability. H9C2 cells were seeded in 96-well plate in triplicate and performed according to the experimental protocol. After washed twice by PBS (Gibco, California, US), each well was added 10ul CCK8 solution in new medium. The absorbances of 450nm and 600nm were measured by multimode reader (Synergy H1, Biotek, US) after 2h in a humidified incubator at 37°C.

# Measurement of cardiomyocyte surface area

H9c2 cells were stained with actin-stain 555 fluorescent phalloidin (PHDH1, cytoskeleton, US) for measure surface area. Cells were seeded on coverslips in 24-well plate. After fixation and permeabilization, cells were incubated with phalloidin for 30 minutes in the dark. The nuclei were stained with 4',6-diamidino-2-phenylindole (DAPI, Beyotime Biotechnology, Shanghai, China). Rinsing the coverslip in PBS and inverting on a drop of anti-fade mounting media (H-1000-10, Vector labs, California, US) on a glass slide were performed. Cell surface areas were determined with Image Pro Plus 6.0.

# Detection of intracellular ROS

The intracellular ROS level were measured by 2',7'-dichlorofluorescin diacetate (DCFH-DA, D6883, Sigma-Aldrich, US) according to the manufacturer's instructions. H9C2 were seeded in 24-well plate. After removed the original culture solution, the wells were washed with PBS twice. DCFH-DA, dissolved with DMSO (D2650, Sigma-Aldrich, US) to a final concentration of 10ng/ml, was added 10ul per well and incubated at 37°C in the dark for 20min. Cells were washed three times using PBS. Subsequently, Fluorescence was monitored by invert fluorescence microscope (Leica, Germany) and photographed. The average optical density of ROS was measured using Image J.

# Hoechst 33342 staining

The apoptotic nucleuses were observed with Hoechst33342. Cell culture and groups were the same as DCFH-DA treatment. Cells were fixed with 4% paraformaldehyde for 20 minutes and the plates were washed 3 times with PBS for 5 minutes each time. 10ul of Hoechst33342 (B2261, Sigma-Aldrich, US, 200ug/ml in PBS,) was added to each well and incubated 5 minutes in the dark. Finally, anti-fade mounting media was used to seal the coverslips. Staining was observed in the fluorescence microscopy.

# Total RNA extracted and quantitative real-time polymerase chain reaction analysis

Total RNA was extracted with TRIzol reagent (15596026, Invitrogen, Thermo Scientific, Massachusetts, US) following the manual and DNA was generated by RevertAid First Strand cDNA Synthesis Kit (K1622, thermo scientific, Massachusetts, US). Quantitative real-time PCR was performed by SYBR green PCR master mix (D7260, Beyotime Biotechnology, Shanghai, China) on CFX96 instrument. The reaction procedure was as follows: heating at 95°C for 5minutes and magnification over 40 cycles of 95°C for 15seconds, 60°C for 30seconds and 95°C for 15 seconds. The primer sequence was as follows:

Myh7 Forward: CCAGAACACCAGCCTCATCAACC

Myh7 Reverse: CACCGCCTCCTCCACCTCTG

Nfe2l2 Forward: GCCTTCCTCTGCTGCCATTAGTC

Nfe2l2 Reverse: TGCCTTCAGTGTGCTTCTGGT TG

Hmox1 Forward: AGGAGATAGAGCGAAACAAGCAGAAC

Hmox1 Reverse: GCTGTGTGGCTGGTGTGTAAGG

Nqo1 Forward: GCTTCTGTGGCTTCCCAGGTC

Nqo1 Reverse: CGCTTCTTCCACCCTTCCAG

The expression of GAPDH was used as the control.

# Western Blotting

Equal protein form cardiac tissue and H9C2 cells were loaded onto the SDS-PAGE gel, prepared according to the kit, and transferred to the polyvinylidene fluoride (PVDF) membrane (Millipore, Massachusetts, US). Then, the membrane was incubated with primary antibody against Nrf2 (CST #20733, Massachusetts, US), HO-1 (proteintech 10701, Wuhan, Hubei, China), NQO1 (proteintech 67240, Wuhan, Hubei, China), Caspase-3 (CST #9662, Massachusetts, US), Bcl-2 (sc-7382, Santa Cruz Biotechnology, US), Bax (CST #2772, Massachusetts, US), GAPDH (Cat No.GTX10018, Gene Tex, US) at 4℃ overnight and incubated with HRP-conjugated secondary antibody(CST #7076,#7074Massachusetts, US) for 1 hour. We used gel

imaging analysis system to visualize the protein signal. Image J software was used for semi-quantitative analysis.

# Data statistics and analysis

The experimental data were expressed as mean ± standard error (SEM). Data conform to normal distribution. One-way analysis of variance (ANOVA) was used for statistical analysis. Brown-Forsythe and Welch ANOVA tests were used when variances were not homogeneous (Graphpad Prism 8.0). *P* value less than 0.05 was considered significant difference.

## Results

# Effects of OED on general characteristics and attenuated oxidative stress in diabetic rats

As shown in Table 1, type 2 diabetic rats displayed weight loss and hyperglycemia. In T2DM group, the contents of MDA in tissue were higher than that in the NC group, while, the concentration of SOD was decreased. After four weeks, OED decreased MDA, while elevated SOD.

Table 1
**General characteristics and oxidative stress index. SOD: superoxide dismutase; MDA: malondialdegyde;**

| | NC | T2DM | T2DM + OED |
|---|---|---|---|
| Number | 10 | 8 | 10 |
| Body weight (g) | 336.3 ± 13.84 | 296.4 ± 4.27$^{\#}$ | 312 ± 17.33 |
| Blood glucose (mmol/L) | 4.18 ± 0.7 | 31.96 ± 1.85$^{\#}$ | 27.28 ± 2.86$^{\#}$ |
| MDA (nmol/ml) | 2.28 ± 0.37 | 2.83 ± 0.41$^{\#}$ | 2.61 ± 0.39* |
| SOD (ng/ml) | 3.84 ± 0.23 | 3.61 ± 0.48$^{\#}$ | 4.21 ± 0.73* |
| Value are mean ± SEM, n = 8–10. $^{\#}p < 0.05$ vs normal; *$p < 0.05$ vs T2DM; | | | |

# OED prevented cardiac diastolic dysfunction in diabetic rats

M-mode and PWD echocardiography of NC, T2DM and T2DM + OED group were performed to evaluate systolic and diastolic function individually, and the representative echocardiographic images and data were shown in Fig. 1 and Table 2. There was no significant change in the percentages of LVEF and LVFS among groups. The E/A ratio of NC group was greater than 1, while less than 1 in T2DM group. The E/A ratio of T2DM + OED group was greater than 1 after OED for 4 weeks,which is similar to that in NC group. Furthermore, the indicators represented myocardial hypertrophy and cardiac chamber dilation detected by two-dimensional echocardiography, including IVSd, LVPWd, LAD, LVM and LVM/BW increased apparently

in T2DM group and significantly decreased in T2DM + OED group. Besides, LVPWs significantly decreased in T2DM + OED group. We also observed that LVIDd and LVIDs increased slightly in diabetic cardiomyopathy and improved after OED treatment.

**Figure 1 Representative echocardiographic images of the left ventricle.**

(a-c) M-mode echocardiography of NC, T2DM and T2DM + OED group were performed to evaluated systolic function by measured left ventricular ejection fraction and left ventricular fractional shortening. (d-f) PWD echocardiography imaging of NC, T2DM and T2DM + OED group were performed to evaluated diastolic function. transthoracic motion mode echocardiography (M-mode), pulsed-wave Doppler echocardiography (PWD); early diastolic peak velocity (E); late diastolic peak velocity (A);

Table 2
**Echocardiographic assessments of cardiac structure and function.**

| | NC | T2DM | T2DM + OED |
|---|---|---|---|
| HR (bpm) | 334.00 ± 2.94 | 343.67 ± 14.82 | 335 ± 23.11 |
| E (cm/s) | 0.59 ± 0.10 | 0.67 ± 0.12 | 0.83 ± 0.19 |
| A (cm/s) | 0.33 ± 0.08 | 0.94 ± 0.11$^{\#}$ | 0.64 ± 0.24 |
| E/A | 1.89 ± 0.43 | 0.70 ± 0.075$^{\#}$ | 1.39 ± 0.33* |
| LVIDd (mm) | 6.24 ± 0.77 | 6.41 ± 0.88 | 6.25 ± 0.63 |
| LVIDs (mm) | 3.33 ± 0.19 | 3.82 ± 0.26 | 3.34 ± 0.09 |
| LVEF (%) | 80.40 ± 6.15 | 79.00 ± 6.10 | 80.00 ± 6.24 |
| LVFS (%) | 43.80 ± 6.05 | 43.00 ± 6.00 | 43.67 ± 5.99 |
| IVSd (mm) | 1.32 ± 0.03 | 1.52 ± 0.14$^{\#}$ | 1.28 ± 0.01* |
| IVSs (mm) | 2.02 ± 0.20 | 2.07 ± 0.12 | 2.03 ± 0.25 |
| LVPWd (mm) | 1.37 ± 0.05 | 1.63 ± 0.05$^{\#}$ | 1.38 ± 0.10* |
| LVPWs (mm) | 1.96 ± 0.22 | 2.10 ± 0.14 | 1.71 ± 0.18* |
| LAD (mm) | 4.82 ± 0.10 | 5.40 ± 0.24$^{\#}$ | 4.57 ± 0.29* |
| LVM (g) | 1.01 ± 0.08 | 1.29 ± 0.13$^{\#}$ | 0.98 ± 0.08* |
| LVM/BW (%) | 0.22 ± 0.01 | 0.29 ± 0.02$^{\#}$ | 0.23 ± 0.02* |

heart rates (HR); early diastolic peak velocity (E)；late diastolic peak velocity (A); ratio of E and A (E/A); left ventricular internal dimension in diastole (LVIDd) ；left ventricular internal dimension in systole (LVIDs)； left ventricular ejection fraction of left ventricular (LVEF)； left ventricular fractional shortening of left ventricular (LVFS); interventricular septal thickness in diastole (IVSd)；interventricular septal thickness in systole (IVSs)；left ventricular posterior wall thickness at end diastole (LVPWd) ；left ventricular posterior wall thickness at end systole (LVPWs); left atrial diameter (LAD); left ventricular mass (LVM); body weight (BW)；Value are mean ± SEM, n = 8–10. $^{\#}p < 0.05$ vs normal; *$p < 0.05$ vs T2DM;

# OED decreased cardiomyocyte hypertrophy and apoptosis in diabetic rats

Histological examination by HE staining showed that the cross-sectional area of cardiomyocytes was significantly increased and the mRNA relative expression of β-MHC was elevated in the T2DM group. Oral administration of OED for 4 weeks prevented the changes (Fig. 2a-c, g, h). Compared to the NC group, TUNEL staining of myocardium in the T2DM group revealed a significant increase in apoptotic index (Fig. 2d-f, i). At the same time, the protein expressions of Caspase3, Bax and Bax/Bcl-2 increased and

bcl2 decreased (Fig. 2j-n). OED significantly reduced the proportion of apoptosis cells and reverse the expression changes of Caspase, Bax and Bcl-2 (Fig. 2j-n).

**Figure 2. OED decreased cardiomyocyte hypertrophy and apoptosis.**

(a-c). Hematoxylin and eosin staining of myocardium (magnification x400, scale bar 50um). (d-f). Terminal deoxynucleotidyl transferase-mediated dUTP nick end-labeling of myocardium (magnification x400, scale bar 50um). Both of HE and TUNEL were taken three views randomly from each tissue sample for calculation. g. The cross-sectional areas of 10 cardiomyocytes were measured randomly in each field and the average value was included in the statistics. h. The relative mRNA expression of β-MHC, calculated against GAPDH. i. Quantitative analysis of TUNEL. The cell nucleus was stained by TUNEL as positive, and the apoptosis rate was determined by the ratio of the positive cells and the total cell number. j-n. Expression levels and quantitative analysis of apoptotic (Caspase3, Bax) and anti-apoptotic (Bcl-2) proteins. The expression of GAPDH was used as the control. Value are mean ± SEM, n = 8–10. $^{\#}p < 0.05$ vs normal; $^{*}p < 0.05$ vs T2DM;

# OED attenuated diabetic myocardial fibrosis

Figure 3 shows representative myocardial histological sections of the three study groups. Compared with the NC group, collagen volume fractions (Fig. 3a-c, j) and the protein expression levels of collagen I/III were increased in the T2DM groups, while significantly reduced after OED treatment (Fig. 3d-i, k, l).

**Figure3. OED attenuated diabetic myocardial fibrosis.**

(a-c). Masson's staining of myocardium (magnification x200, scale bar 100um). (d-i). Immunohistochemistry of collagen I and III (magnification x200, scale bar 100um). Each sample was taken three views for statistic. (j-l). Data are expressed as the mean ± SEM, n = 8–10. $^{\#}p < 0.05$ vs normal; $^{*}p < 0.05$ vs T2DM;

# OED activated Nrf2 pathway in myocardial tissue of diabetic rats

The mRNA expression levels of Nrf2, HO-1 and NQO1 were up-regulation in the T2DM group. After OED treatment for four weeks, the mRNA expressions of Nrf2, HO-1 and NQO1 were further increased (Fig. 4a-c). Western blotting revealed that OED significantly increased the protein expression levels of Nrf2, HO-1 and NQO1 in diabetes (Fig. 4d-g). Cytoplasmic Nrf2 was obviously increased in both the T2DM and T2DM + OED groups compared with the normal group (Fig. 4h, i). Nuclear Nrf2 expression in the T2DM + OED group was significantly higher than that in the NC and T2DM group (Fig. 4h, j).

**Figure4. OED activated Nrf2 pathway in diabetic rats.**

(a-c) The mRNA expression levels of Nrf2, HO-1 and NQO1 were evaluated by quantitative real-time polymerase chain reaction analysis, calculated against GAPDH. (d) The protein expression levels of Nrf2, HO-1 and NQO1 were evaluated by western blotting. (e-g) Quantitative analysis of protein expression

levels of Nrf2, HO-1 and NQO1. (h) The protein expression levels of nuclear and cytoplasmic Nrf2 were evaluated by western blotting. (i-j) Quantitative analysis of protein expression levels of nuclear and cytoplasmic Nrf2. The protein expression of GAPDH was used as the control of total and cytoplasmic protein and Lamin B as the nuclear protein. $^{\#}p < 0.05$ vs normal; $^{*}p < 0.05$ vs T2DM;

**Oral edaravone attenuated ROS production, cardiomyocyte hypertrophy and apoptosis via Nrf2 pathway in glucolipotoxicity-induced H9C2 cells**

OED significantly decreased the levels of ROS, cell surface areas and apoptosis ratio induced by high glucose and high fat in H9C2 cardiomyocytes (Fig. 5a-d). The therapeutic effect of OED was eliminated after silencing Nrf2 (Fig. 5a-d).

**Figure5. The effects of OED attenuating HG/HF-Induced cardiomyocyte hypertrophy, reactive oxygen species and apoptosis could be canceled by silencing Nrf2.**

(a) Images and analysis of ROS detected by DCFH-DA. (magnification x100, scale bar 100um) (b) Images and analysis of cell surface area by F-actin stained with fluorescent phalloidin and DAPI counterstained nuclei. (magnification x400, scale bar 20um) (c) Images of apoptotic nuclei presented by Hoechst33342. (magnification x200, scale bar 50um). (d) Images and analysis of apoptotic nuclei detected by TUNEL. (magnification x100, scale bar 100um). Three views were taken randomly from each coverslip for calculation. Data are mean ± SEM of three independent experiments.

# Oral edaravone increased cardiomyocyte viability via Nrf2 pathway in glucolipotoxicity-induced H9C2 cells

The mRNA and protein expression levels of Nrf2 were significantly decreased after NRF2 siRNA transfection in H9C2 cells (Fig. 6a-c). OED was harmless to H9C2 cells at different concentrations (Fig. 6d). The protective effect of OED for HG/HF-induced H9C2 was gradually increased at different concentrations (Fig. 6e). The effect was inhibited by Nrf2 silencing (Fig. 6f). The mRNA expression level of β-MHC was increased (Fig. 6g). The mRNA expression level of NQO1 and HO-1 were decreased in HG/HF-induced H9C2 (Fig. 6i, j). After incubated with OED for 48h, the mRNA expression levels of β-MHC was decreased (Fig. 6g). The mRNA expression levels Nrf2, NQO1 and HO-1 were increased (Fig. 6h-j). OED remarkably increased the protein expression levels of Nrf2, HO-1 and NQO1 in diabetes (Fig. 6k-n). Nrf2 gene silencing abolished the activation of Nrf2 pathway induced by OED and decreased the content of NQO1 and HO-1 (Fig. 6h-n). The expression level of cytoplasmic Nrf2 was increased slightly in HG/HF group (Fig. 6o, p). The expression level of nuclear Nrf2 in the HG/HF + OED group was significantly higher than that in HG/HF group (Fig. 6o, q).

**Figure6. OED attenuated H9C2 cardiomocytes injured by HG/HF via Nrf2 pathway.**

(a-c) Effect of Nrf2 siRNA transfection in H9C2, which detected by RT-qPCR and western blotting; (d) Viability of H9C2 cells after incubated with OED at different concentrations (ug/l) for 48h; (e) Effect of OED at different concentrations on HG/HF-induced damage in H9C2 cells. (f) Effect of OED on HG/HF-

induced damage in H9C2 cells with or without siNrf2 transfection. (g-j) The mRNA expression levels of β-MHC, Nrf2, NQO1and HO-1 were evaluated by quantitative real-time polymerase chain reaction analysis, calculated against GAPDH. (k) The protein expression levels of Nrf2, HO-1 and NQO1 were evaluated by western blotting. (l-n) Quantitative analysis for the protein levels of Nrf2, NQO1 and HO-1. (o) The protein expression levels of nuclear and cytoplasmic Nrf2 were evaluated by western blotting. (p, q) Quantitative analysis for the protein levels of nuclear and cytoplasmic Nrf2. The protein expression of GAPDH was used as the control of total and cytoplasmic protein and Lamin B as the nuclear protein. $^{\#}p < 0.05$ vs normal; $^{*}p < 0.05$ vs T2DM;

# Discussion

The present study revealed that OED ameliorated the diastolic dysfunction of diabetic cardiomyopathy, as evidenced by alleviating cardiomyocyte hypertrophy, apoptosis, extracellular matrix protein deposition and myocardial interstitial fibrosis induced by oxidative stress. These effects were likely achieved by activating the Nrf2 signaling pathway. Our study also demonstrated that OED protected H9C2 from glucolipotoxity, and the underlying mechanism involves Nrf2 activation. However, the protective effects of OED in cardiomyocytes were cancelled by Nrf2 silence.

Clinical course of DCM develops from diastolic dysfunction to severe diastolic heart failure with normal ejection fraction, and finally leads to heart failure with reduced ejection fraction[7,30,31]. Left ventricular diastolic dysfunction is very common in asymptomatic diabetic patients, and at least 50% diabetes mellitus has left ventricular diastolic dysfunction[6,8]. However, there is no effective clinical management on diastolic dysfunction. Excessive ROS induced by hyperglycemia and hyperlipidemia has been the main cause of diastolic dysfunction in diabetic cardiomyopathy[10]. Previous studies confirmed that antioxidant therapy improved oxidative stress in diabetic myocardium[32]. Our study showed that the diabetic rats got diastolic dysfunction without decrease in ejection fraction, which was consistent in the early manifestation of DCM. The OED treatment for four weeks improved significantly the diastolic dysfunction. OED alleviates the pathophysiological alterations of DCM, including myocardial remodeling and stiffness increase[8,33], which mainly induced by cardiac hypertrophy, myocardial apoptosis, collagen deposition, and interstitial fibrosis[3].

Myocardial hypertrophy is the earliest visible structural change in DCM[2], and cardiomyocyte hypertrophy is the major reason[34]. Oxidative stress leads to the increase in protein synthesis in cardiomyocytes and produces new sarcomeres, which induces larger cardiomyocyte transverse diameter[35]. Meanwhile, oxidative stress cooperating with insulin resistance and hyperglycemia produces fetal proteins such as β-Myosin heavy chain (β-MHC), which is normally expressed in adult myocardium and stimulates pathological cardiomyocyte hypertrophy[6]. Moreover, ROS is able to target sarcomeric proteins and affect post-translational modifications of the elastic filament protein titin to increase cardiomyocyte stiffness[36,37]. In this study, there are indicators of cardiac hypertrophy such as left ventricular wall thickness,inter-ventricular septum thickness, left atrial diameter and left ventricular mass significantly

increased in diabetic rats, whereas these parameters were decreased after OED treatment. OED also reduced the volume of cardiomyocytes and its expression of β-MHC. On the other hand, pathological cardiac hypertrophy in diabetic myocardium is distinguished from physiological cardiac hypertrophy of athletes and pregnant women[38]. In addition to the enlarged volume of cardiomyocyte, apoptosis is another feature of pathological hypertrophy[39]. The number of cardiomyocytes decreases due to apoptosis is also an important reason for myocardial dysfunction. Oxidative stress plays an important role in cell apoptosis with diabetic cardiomyocytes and DNA fragmentation induced by ROS is a prominent character of cell apoptosois[40]. The effect of OED attenuating oxidative stress further inhibited cardiomyocyte apoptosis. OED obviously reduced the proportion of apoptotic cells in vivo and in vitro, thereby alleviating myocardial dysfunction in diabetes.

The increase in the extracellular volume is another important reason for diastolic dysfunction in diabetes[13]. The extracellular volume increase, including deposition of collagen and formation of interstitial fibrosis[41], induces myocardial stiffness followed by diastolic dysfunction[42]. Cardiac fibroblasts maintain homeostasis of the cardiac extracellular matrix under physiological circumstances by synthesizing small amounts of collagen[43]. Oxidative stress leads to the activation of fibroblasts and increases extracellular matrix synthesis, which ultimately directly promotes interstitial collagen deposition[13]. Recent studies on cardiac remodeling have identified that abnormal fibroblasts are resistant to apoptosis and caused formation of abnormal cardiac matrix in HFpEF [44]. On the other hand, ROS increases the production of advanced glycation end products (AGEs), to promote fibroblast differentiation into myofibroblasts and exacerbate the formation of myocardial fibrosis, collagen expression and cross-linking[45]. Clinical research also revealed the accumulation of collagen type I and type III in the cardiac interstitium of T2DM patients[46]. Therefore, anti-fibrotic therapy becomes an effective measure to improve diastolic dysfunction of the myocardium[47]. In our study, the interstitial collagen deposition in diabetic myocardium was significantly higher than that in normal myocardium. To further investigate the formation of myocardial fibrosis, Masson staining revealed that myocardial interstitial fibrosis increased obviously. After OED treatment, collagen accumulation and interstitial fibrosis were improved significantly, which is another reason for OED improving myocardial diastolic function in diabetes.

In order to further explore the molecular mechanism of OED on antioxidant effect in DCM, we focused on Nrf2 signal pathway. Nrf2 is an important endogenous antioxidant regulator, which protects cell components such as protein and DNA from oxidative stress injury[48]. Nrf2 maintains low activity in the physiological state. When stimulated by ROS, Nrf2 dissociates from its inhibitor epoxy chloropropane Kelch sample related protein-1 (Keap1) and occurs on nuclear translocation [49]. Imbalance of redox homeostasis changes myocardial structure and function, resulted in pathologic hypertrophy, fibrosis and cardiac dysfunction in diabetes. NRF2 plays an important role in attenuating the pathophysiological process and cardiac dysfunction induced by oxidative stress in diabetes[26,50]. The mRNA expression level of β- MHC increased and accelerated the development of heart failure in Nrf2 knockout mice.[51] Nrf2 knockout mice are more susceptible to hyperglycemia-induced cardiomyopathy and cell death than wild-

type ones[52] and the LV diastolic dysfunction mainly referable to cardiac hypertrophy and down-regulation of SERCA2a rather than alterations in coronary artery function or systemic hemodynamics[53]. As an important protective factor, NRF2 is reactively increased in the early phase of diabetic myocardium, but significantly decreased in the advanced phase[54,55]. Previous studies show that Nrf2 inducer improves diabetic oxidative stress injury and a variety of natural or synthetic NRF2 activators have ideal therapeutic effects on DCM[56,57]. Consequently, NRF2 has become a potential effective therapy target for the treatment of DCM[58]. In the experiment, we observed that the expression of NRF2 was increased significantly after OED treatment. OED might act as a NRF2 agonist to increase the expression of antioxidant enzymes and protect the myocardium from oxidative damage. Moreover, we observed that the expression level of Nrf2 was increased in diabetic rats, which was compatible with the early alteration of diabetes in previous studies. However, diabetes-induced increase of Nrf2 expression was located in the cytoplasm rather than nuclear translocation, which was necessary for effective antioxidant protection. After OED treatment, both cytoplasmic and nuclear Nrf2 were increased. Furthermore, nuclear Nrf2 increased significantly and then exerted an antioxidant effect. The antioxidant activity of Nrf2 is mediated by NADPH quinone oxidoreductase (NQO1) and heme oxygenase (HO-1) [27]. Consistently we found that the mRNA and protein expression levels of NQO1 and HO-1 were increased in vivo and in vitro after OED treatment. Finally, we showed that the effect of OED on improving oxidative damage in H9c2 cells injured was lost after silencing Nrf2, suggesting that the protective effect of OED on cardiomyocytes is at least partially via activating the Nrf2 pathway. Our study confirmed that OED can attenuate the diabetic cardiomyopathy possibly via activating Nrf2 pathway. However, researches have reported that Nrf2 activation may depend on evaluating the upstream signaling pathways, such as PI3K[59], β-RECP[60], SIRT1[61]and GSKβ[54]. It requires experimental validation that whether OED activates the upstream signaling pathways to further affect Nrf2 or not.

Our study had several limitations as follows. Firstly, for better investigate the effect of OED on diastolic function, we observed type 2 diabetic rats for only 4 weeks to develop only diastolic dysfunction without systolic dysfunction, and whether OED have influence on systolic dysfunction in diabetic cardiomyopathy cannot be determined. Secondly, although OED exhibited protective effects on the myocardium both in vivo and in vitro, high glucose and high-fat injuries in animal and cell models were not synchronized. The efficacy of OED on different diabetic myocardial stages needs to be set more time points for corroboration. At last, as myocardial collagen accumulation and interstitial fibrosis are important pathological changes causing cardiac dysfunction, the ameliorative effect of OED on this mechanism needs further explored using cardiac fibroblasts in vitro. We will continue to refine these points in subsequent studies.

# Conclusion

OED improved hypertrophy, apoptosis of cardiomyocytes and myocardial fibrosis, eventually relieving diabetic myocardial diastolic dysfunction, which associated with alleviated oxidative stress injury by activating Nrf2 signaling pathway. Novel OED has the potential to be an Nrf2 agonist for clinical

treatment of diabetic cardiomyopathy. Edaravone is only available as the injection formula, which is not suitable for the chronic condition of DCM. Our study provides a potential therapeutic agent which the novel oral formula for future clinical trial to treat chronic diabetic cardiomyopathy.

# Abbreviations

DCM: diabetic cardiomyopathy; OED: Oral-edaravone; STZ: streptozotocin; MDA: malondialdehyde; SOD: superoxide dismutase; ROS: reactive oxygen species; DM: diabetes mellitus; ED: Edaravone; AD: Alzheimer'sdisease; Nrf2: Nuclear factor erythroid-derived 2 like 2; Keap1: Kelch sample related protein-1; NQO1: nicotinamide adenine dinucleotide phosphate quinone oxidoreductase; HO-1: heme oxygenase; M-mode: motion mode; PWD: pulsed-wave Doppler; HR: heart rates; E velocity: early diastolic peak velocity; A velocity: late diastolic peak velocity; LVIDd: left ventricular internal dimension ; LVIDs: left ventricular internal dimension in systole; IVSd: interventricular septal thickness in diastole; IVSs: interventricular septal thickness in systole; LVPWd: left ventricular posterior wall thickness at end diastole; LVPWs: left ventricular posterior wall thickness at end systole; LAD: left atrial diameter; LVEF: left ventricular ejection fraction; LVFS: left ventricular fractional shortening; E/A ratio: ratio of E and A velocity; LVM: left ventricular mass; LVW/BW: ratio of left ventricular mass and body weight ; β-MHC: β-Myosin heavy chain; AGEs: advanced glycation end products.

# Declarations

### Ethics approval and consent to participate

The animal experiments were approved by the Animal Research Ethics Committee of Kunming Medical University.

### Consent for publication

All authors declare their consent for this publication.

### Availability of data and materials

The datasets used and analysed during the current study are available from the corresponding author on reasonable request.

### Competing interest

The authors declare that they have no competing interest.

### Funding

This work was supported by Grants from Applied Basic Program of Yunnan Clinical Medical Center for Heart and Cerebrovascular Diseases (No. ZX2019-03-01).

### Authors' Contributions

LW, YQZ and LJP designed the study; LW, JHG, RS and PHC conducted the experiments. YQZ, YXX and XXS performed the statistical analysis; LW, XFZ and LHY drafted the manuscript; LJP, HYL and XFZ revised the manuscript. All authors read and approved the final manuscript.

### Acknowledgements

Thank you for our colleagues in Biomedical Engineering Research Center of Kunming Medical University and First Affiliated Hospital of Kunming Medical University.

### Authors' information

[1] Department of Cardiology, First Affiliated Hospital of Kunming Medical University,

Kunming, China.

[2] Yunnan Key Laboratory of Stem Cells and Regeneration Medicine, Biomedical Engineering Research Center, Kunming Medical University, Kunming, China.

[3] Department of Ultrasound, Second Affiliated Hospital of Kunming Medical University, Kunming, China.

[4] Department of Pharmacology, College of Basic Medicine, Kunming Medical University, Kunming China

[5] Health and Biomedical Innovation, Clinical and Health Sciences, University of South Australia, Adelaide, Australia

# References

1. Dillmann WH. Diabetic Cardiomyopathy. *Circ Res* 2019;124:1160–1162.
2. Nikolajevic Starcevic J, Janic M, Sabovic M. Molecular Mechanisms Responsible for Diastolic Dysfunction in Diabetes Mellitus Patients. *Int J Mol Sci* 2019;20.
3. Jia G, Whaley-Connell A, Sowers JR. Diabetic cardiomyopathy: a hyperglycaemia- and insulin-resistance-induced heart disease. *Diabetologia* 2018;61:21–28.
4. Falcão-Pires I, Leite-Moreira AF. Diabetic cardiomyopathy: understanding the molecular and cellular basis to progress in diagnosis and treatment. *Heart Fail Rev* 2012;17:325–344.
5. Zhang X, Zhang Z, Yang Y, Suo Y, Liu R, Qiu J, Zhao Y, Jiang N, Liu C, Tse G, Li G, Liu T. Alogliptin prevents diastolic dysfunction and preserves left ventricular mitochondrial function in diabetic rabbits. *Cardiovasc Diabetol* 2018;17:160.
6. Jia G, Hill MA, Sowers JR. Diabetic Cardiomyopathy: An Update of Mechanisms Contributing to This Clinical Entity. *Circ Res* 2018;122:624–638.

7. Evangelista I, Nuti R, Picchioni T, Dotta F, Palazzuoli A. Molecular Dysfunction and Phenotypic Derangement in Diabetic Cardiomyopathy. *Int J Mol Sci* 2019;20.
8. Marwick TH, Ritchie R, Shaw JE, Kaye D. Implications of Underlying Mechanisms for the Recognition and Management of Diabetic Cardiomyopathy. *J Am Coll Cardiol* 2018;71:339–351.
9. Sies H, Jones DP. Reactive oxygen species (ROS) as pleiotropic physiological signalling agents. *Nat Rev Mol Cell Biol* 2020;21:363–383.
10. Forrester SJ, Kikuchi DS, Hernandes MS, Xu Q, Griendling KK. Reactive Oxygen Species in Metabolic and Inflammatory Signaling. *Circ Res* 2018;122:877–902.
11. Kaludercic N, Di Lisa F. Mitochondrial ROS Formation in the Pathogenesis of Diabetic Cardiomyopathy. *Front Cardiovasc Med* 2020;7:12.
12. Guo R, Wu Z, Jiang J, Liu C, Wu B, Li X, Li T, Mo H, He S, Li S, Yan H, Huang R, You Q, Wu K. New mechanism of lipotoxicity in diabetic cardiomyopathy: Deficiency of Endogenous H(2)S Production and ER stress. *Mech Ageing Dev* 2017;162:46–52.
13. Tan Y, Zhang Z, Zheng C, Wintergerst KA, Keller BB, Cai L. Mechanisms of diabetic cardiomyopathy and potential therapeutic strategies: preclinical and clinical evidence. *Nat Rev Cardiol* 2020;17:585–607.
14. Huynh K, Bernardo BC, McMullen JR, Ritchie RH. Diabetic cardiomyopathy: mechanisms and new treatment strategies targeting antioxidant signaling pathways. *Pharmacol Ther* 2014;142:375–415.
15. Wan YJ, Hu L, Wang XM. Edaravone protects from retinal injury through NF-κB in diabetic rats. *Eur Rev Med Pharmacol Sci* 2019;23:17–23.
16. Yuan D, Xu Y, Hang H, Liu X, Chen X, Xie P, Yuan S, Zhang W, Lin X, Liu Q. Edaravone protect against retinal damage in streptozotocin-induced diabetic mice. *PLoS One* 2014;9:e99219.
17. Fan Y, Wu W, Lei Y, Gaucher C, Pei S, Zhang J, Xia X. Edaravone-Loaded Alginate-Based Nanocomposite Hydrogel Accelerated Chronic Wound Healing in Diabetic Mice. *Mar Drugs* 2019;17.
18. Varatharajan R, Lim LX, Tan K, Tay CS, Teoh YL, Akhtar SS, Rupeshkumar M, Chung I, Abdullah NA, Banik U, Dhanaraj SA, Balakumar P. Effect of edaravone in diabetes mellitus-induced nephropathy in rats. *Korean J Physiol Pharmacol* 2016;20:333–340.
19. Jiao SS, Yao XQ, Liu YH, Wang QH, Zeng F, Lu JJ, Liu J, Zhu C, Shen LL, Liu CH, Wang YR, Zeng GH, Parikh A, Chen J, Liang CR, Xiang Y, Bu XL, Deng J, Li J, Xu J, Zeng YQ, Xu X, Xu HW, Zhong JH, Zhou HD, Zhou XF, Wang YJ. Edaravone alleviates Alzheimer's disease-type pathologies and cognitive deficits. *Proc Natl Acad Sci U S A* 2015;112:5225–5230.
20. Parikh A, Kathawala K, Song Y, Zhou XF, Garg S. Curcumin-loaded self-nanomicellizing solid dispersion system: part I: development, optimization, characterization, and oral bioavailability. *Drug Deliv Transl Res* 2018;8:1389–1405.
21. Parikh A, Kathawala K, Tan CC, Garg S, Zhou XF. Lipid-based nanosystem of edaravone: development, optimization, characterization and in vitro/in vivo evaluation. *Drug Deliv* 2017;24:962–978.

22. Hybertson BM, Gao B, Bose SK, McCord JM. Oxidative stress in health and disease: the therapeutic potential of Nrf2 activation. *Mol Aspects Med* 2011;32:234–246.
23. Yu H, Wu Z, Wang X, Gao C, Liu R, Kang F, Dai M. Protective effects of combined treatment with mild hypothermia and edaravone against cerebral ischemia/reperfusion injury via oxidative stress and Nrf2 pathway regulation. *Int J Oncol* 2020;57:500–508.
24. Zhang J, Shi X, Chen Z, Geng J, Wang Y, Feng H, Zhu G, Chen Q. Edaravone Reduces Iron-Mediated Hydrocephalus and Behavioral Disorder in Rat by Activating the Nrf2/HO-1 Pathway. *J Stroke Cerebrovasc Dis* 2018;27:3511–3520.
25. Pan Y, Li W, Feng Y, Xu J, Cao H. Edaravone attenuates experimental asthma in mice through induction of HO-1 and the Keap1/Nrf2 pathway. *Exp Ther Med* 2020;19:1407–1416.
26. Chen QM, Maltagliati AJ. Nrf2 at the heart of oxidative stress and cardiac protection. *Physiol Genomics* 2018;50:77–97.
27. Bellezza I, Giambanco I, Minelli A, Donato R. Nrf2-Keap1 signaling in oxidative and reductive stress. *Biochim Biophys Acta Mol Cell Res* 2018;1865:721–733.
28. Bai Y, Cui W, Xin Y, Miao X, Barati MT, Zhang C, Chen Q, Tan Y, Cui T, Zheng Y, Cai L. Prevention by sulforaphane of diabetic cardiomyopathy is associated with up-regulation of Nrf2 expression and transcription activation. *J Mol Cell Cardiol* 2013;57:82–95.
29. Skovso S Modeling type 2 diabetes in rats using high fat diet and streptozotocin. *J Diabetes Investig* 2014;5:349–358.
30. Paolillo S, Marsico F, Prastaro M, Renga F, Esposito L, De Martino F, Di Napoli P, Esposito I, Ambrosio A, Ianniruberto M, Mennella R, Paolillo R, Gargiulo P. Diabetic Cardiomyopathy: Definition, Diagnosis, and Therapeutic Implications. *Heart Fail Clin* 2019;15:341–347.
31. Tarquini R, Pala L, Brancati S, Vannini G, De Cosmo S, Mazzoccoli G, Rotella CM. Clinical Approach to Diabetic Cardiomyopathy: A Review of Human Studies. *Curr Med Chem* 2018;25:1510–1524.
32. Li K, Zhai M, Jiang L, Song F, Zhang B, Li J, Li H, Li B, Xia L, Xu L, Cao Y, He M, Zhu H, Zhang L, Liang H, Jin Z, Duan W, Wang S. Tetrahydrocurcumin Ameliorates Diabetic Cardiomyopathy by Attenuating High Glucose-Induced Oxidative Stress and Fibrosis via Activating the SIRT1 Pathway. *Oxid Med Cell Longev* 2019;2019:6746907.
33. van Heerebeek L, Hamdani N, Handoko ML, Falcao-Pires I, Musters RJ, Kupreishvili K, Ijsselmuiden AJ, Schalkwijk CG, Bronzwaer JG, Diamant M, Borbély A, van der Velden J, Stienen GJ, Laarman GJ, Niessen HW, Paulus WJ. Diastolic stiffness of the failing diabetic heart: importance of fibrosis, advanced glycation end products, and myocyte resting tension. *Circulation* 2008;117:43–51.
34. Adeghate E, Singh J. Structural changes in the myocardium during diabetes-induced cardiomyopathy. *Heart Fail Rev* 2014;19:15–23.
35. Martin-Fernandez B, Gredilla R. Mitochondria and oxidative stress in heart aging. *Age (Dordr)* 2016;38:225–238.
36. Grützner A, Garcia-Manyes S, Kötter S, Badilla CL, Fernandez JM, Linke WA. Modulation of titin-based stiffness by disulfide bonding in the cardiac titin N2-B unique sequence. *Biophys J* 2009;97:825–

834.

37. Hopf AE, Andresen C, Kötter S, Isić M, Ulrich K, Sahin S, Bongardt S, Röll W, Drove F, Scheerer N, Vandekerckhove L, De Keulenaer GW, Hamdani N, Linke WA, Krüger M. Diabetes-Induced Cardiomyocyte Passive Stiffening Is Caused by Impaired Insulin-Dependent Titin Modification and Can Be Modulated by Neuregulin-1. *Circ Res* 2018;123:342–355.
38. Cotecchia S, Del Vescovo CD, Colella M, Caso S, Diviani D. The alpha1-adrenergic receptors in cardiac hypertrophy: signaling mechanisms and functional implications. *Cell Signal* 2015;27:1984–1993.
39. Ren Z, Yu P, Li D, Li Z, Liao Y, Wang Y, Zhou B, Wang L. Single-Cell Reconstruction of Progression Trajectory Reveals Intervention Principles in Pathological Cardiac Hypertrophy. *Circulation* 2020;141:1704–1719.
40. Trinei M, Giorgio M, Cicalese A, Barozzi S, Ventura A, Migliaccio E, Milia E, Padura IM, Raker VA, Maccarana M, Petronilli V, Minucci S, Bernardi P, Lanfrancone L, Pelicci PG. A p53-p66Shc signalling pathway controls intracellular redox status, levels of oxidation-damaged DNA and oxidative stress-induced apoptosis. *Oncogene* 2002;21:3872–3878.
41. Aroor AR, Mummidi S, Lopez-Alvarenga JC, Das N, Habibi J, Jia G, Lastra G, Chandrasekar B, DeMarco VG. Sacubitril/valsartan inhibits obesity-associated diastolic dysfunction through suppression of ventricular-vascular stiffness. *Cardiovasc Diabetol* 2021;20:80.
42. Tham YK, Bernardo BC, Ooi JY, Weeks KL, McMullen JR. Pathophysiology of cardiac hypertrophy and heart failure: signaling pathways and novel therapeutic targets. *Arch Toxicol* 2015;89:1401–1438.
43. Baum J, Duffy HS. Fibroblasts and myofibroblasts: what are we talking about? *J Cardiovasc Pharmacol* 2011;57:376–379.
44. Nair N Epidemiology and pathogenesis of heart failure with preserved ejection fraction. *Rev Cardiovasc Med* 2020;21:531–540.
45. Lazo M, Halushka MK, Shen L, Maruthur N, Rebholz CM, Rawlings AM, Hoogeveen RC, Brinkley TE, Ballantyne CM, Astor BC, Selvin E. Soluble receptor for advanced glycation end products and the risk for incident heart failure: The Atherosclerosis Risk in Communities Study. Am Heart J 2015;170:961–7.
46. Shimizu M, Umeda K, Sugihara N, Yoshio H, Ino H, Takeda R, Okada Y, Nakanishi I. Collagen remodelling in myocardia of patients with diabetes. *J Clin Pathol* 1993;46:32–36.
47. Schimmel K, Jung M, Foinquinos A, José GS, Beaumont J, Bock K, Grote-Levi L, Xiao K, Bär C, Pfanne A, Just A, Zimmer K, Ngoy S, López B, Ravassa S, Samolovac S, Janssen-Peters H, Remke J, Scherf K, Dangwal S, Piccoli MT, Kleemiss F, Kreutzer FP, Kenneweg F, Leonardy J, Hobuß L, Santer L, Do QT, Geffers R, Braesen JH, Schmitz J, Brandenberger C, Müller DN, Wilck N, Kaever V, Bähre H, Batkai S, Fiedler J, Alexander KM, Wertheim BM, Fisch S, Liao R, Diez J, González A, Thum T. Natural Compound Library Screening Identifies New Molecules for the Treatment of Cardiac Fibrosis and Diastolic Dysfunction. *Circulation* 2020;141:751–767.
48. Ma Q Role of nrf2 in oxidative stress and toxicity. *Annu Rev Pharmacol Toxicol* 2013;53:401–426.

49. Baird L, Yamamoto M. The Molecular Mechanisms Regulating the KEAP1-NRF2 Pathway. *Mol Cell Biol* 2020;40.
50. Vashi R, Patel BM. NRF2 in Cardiovascular Diseases: a Ray of Hope! *J Cardiovasc Transl Res* 2020.
51. Strom J, Chen QM. Loss of Nrf2 promotes rapid progression to heart failure following myocardial infarction. *Toxicol Appl Pharmacol* 2017;327:52–58.
52. Gu J, Cheng Y, Wu H, Kong L, Wang S, Xu Z, Zhang Z, Tan Y, Keller BB, Zhou H, Wang Y, Xu Z, Cai L. Metallothionein Is Downstream of Nrf2 and Partially Mediates Sulforaphane Prevention of Diabetic Cardiomyopathy. *Diabetes* 2017;66:529–542.
53. Erkens R, Kramer CM, Lückstädt W, Panknin C, Krause L, Weidenbach M, Dirzka J, Krenz T, Mergia E, Suvorava T, Kelm M, Cortese-Krott MM. Left ventricular diastolic dysfunction in Nrf2 knock out mice is associated with cardiac hypertrophy, decreased expression of SERCA2a, and preserved endothelial function. *Free Radic Biol Med* 2015;89:906–917.
54. Xin Y, Bai Y, Jiang X, Zhou S, Wang Y, Wintergerst KA, Cui T, Ji H, Tan Y, Cai L. Sulforaphane prevents angiotensin II-induced cardiomyopathy by activation of Nrf2 via stimulating the Akt/GSK-3ß/Fyn pathway. *Redox Biol* 2018;15:405–417.
55. Luo J, Yan D, Li S, Liu S, Zeng F, Cheung CW, Liu H, Irwin MG, Huang H, Xia Z. Allopurinol reduces oxidative stress and activates Nrf2/p62 to attenuate diabetic cardiomyopathy in rats. *J Cell Mol Med* 2020;24:1760–1773.
56. Ge ZD, Lian Q, Mao X, Xia Z. Current Status and Challenges of NRF2 as a Potential Therapeutic Target for Diabetic Cardiomyopathy. *Int Heart J* 2019;60:512–520.
57. Lian Y, Xia X, Zhao H, Zhu Y. The potential of chrysophanol in protecting against high fat-induced cardiac injury through Nrf2-regulated anti-inflammation, anti-oxidant and anti-fibrosis in Nrf2 knockout mice. *Biomed Pharmacother* 2017;93:1175–1189.
58. Sivasankar D, George M, Sriram DK. Novel approaches in the treatment of diabetic cardiomyopathy. *Biomed Pharmacother* 2018;106:1039–1045.
59. Gao S, Wang R, Dong S, Wu J, Perek B, Xia Z, Yao S, Wang T. Inactivation of TOPK Caused by Hyperglycemia Blocks Diabetic Heart Sensitivity to Sevoflurane Postconditioning by Impairing the PTEN/PI3K/Akt Signaling. *Oxid Med Cell Longev* 2021;2021:6657529.
60. Rada P, Rojo AI, Chowdhry S, McMahon M, Hayes JD, Cuadrado A. SCF/{beta}-TrCP promotes glycogen synthase kinase 3-dependent degradation of the Nrf2 transcription factor in a Keap1-independent manner. *Mol Cell Biol* 2011;31:1121–1133.
61. Ma W, Guo W, Shang F, Li Y, Li W, Liu J, Ma C, Teng J. Bakuchiol Alleviates Hyperglycemia-Induced Diabetic Cardiomyopathy by Reducing Myocardial Oxidative Stress via Activating the SIRT1/Nrf2 Signaling Pathway. *Oxid Med Cell Longev* 2020;2020:3732718.

# Figures

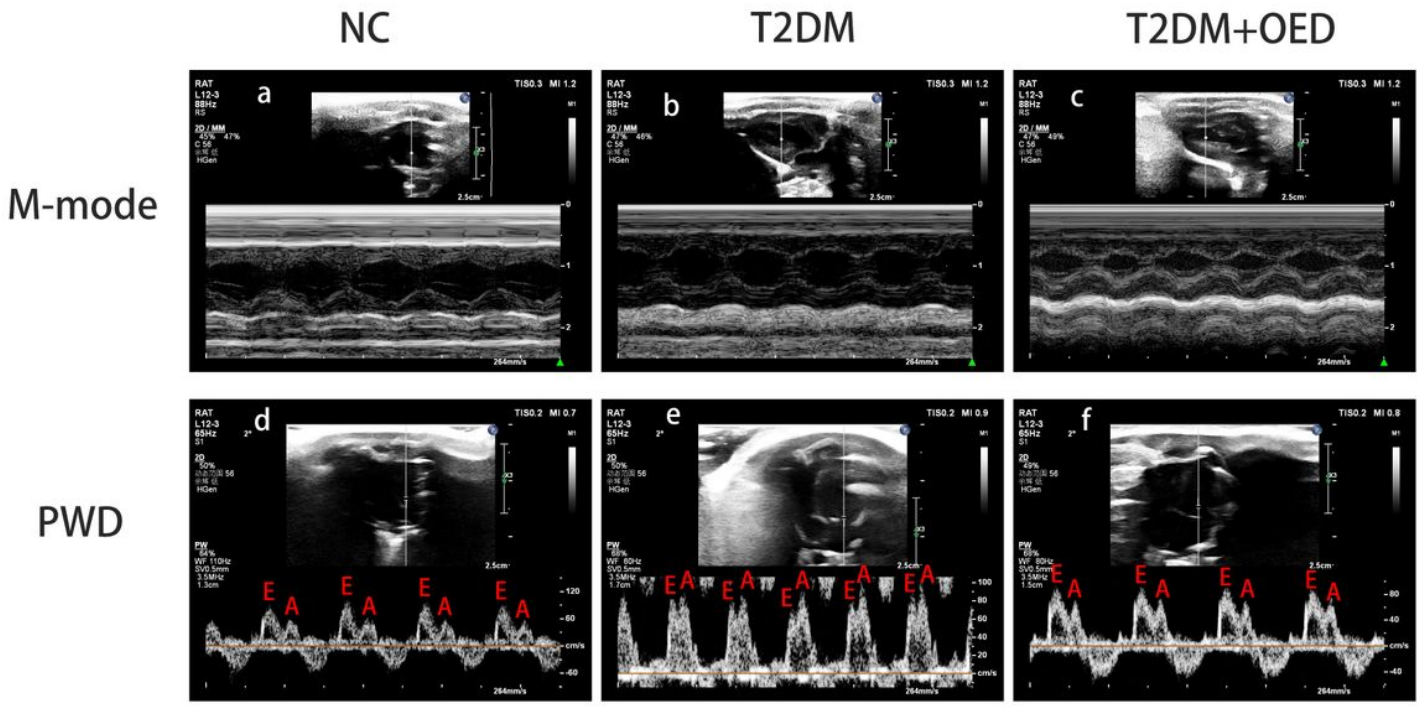


## Figure 1

Representative echocardiographic images of the left ventricle. (a-c) M-mode echocardiography of NC, T2DM and T2DM+OED group were performed to evaluated systolic function by measured left ventricular ejection fraction and left ventricular fractional shortening. (d-f) PWD echocardiography imaging of NC, T2DM and T2DM+OED group were performed to evaluated diastolic function. transthoracic motion mode echocardiography (M-mode), pulsed-wave Doppler echocardiography (PWD); early diastolic peak velocity (E); late diastolic peak velocity (A);

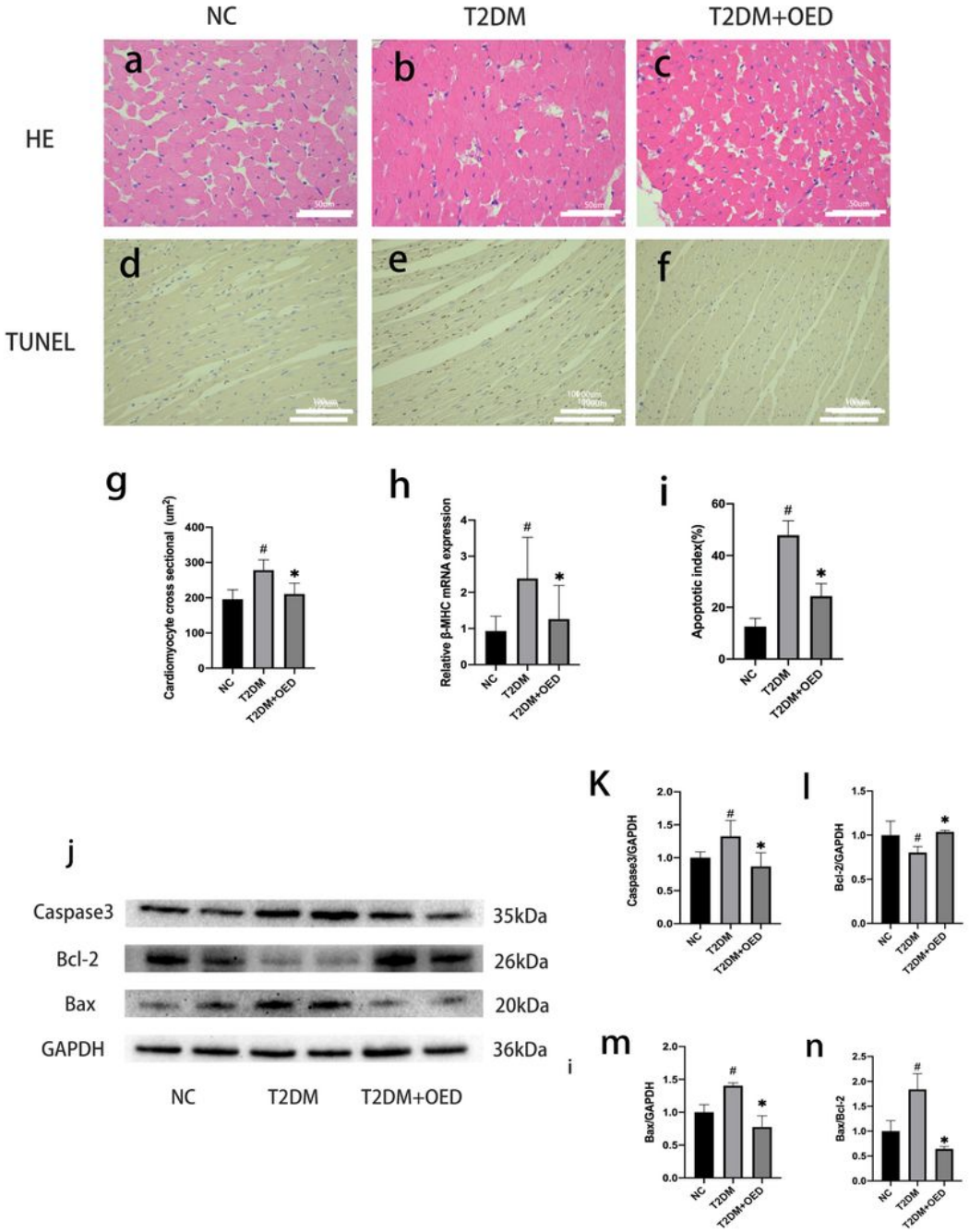


## Figure 2

OED decreased cardiomyocyte hypertrophy and apoptosis. (a-c). Hematoxylin and eosin staining of myocardium (magnification x400, scale bar 50um). (d-f). Terminal deoxynucleotidyl transferase-mediated dUTP nick end-labeling of myocardium (magnification x400, scale bar 50um). Both of HE and TUNEL were taken three views randomly from each tissue sample for calculation. g. The cross-sectional areas of 10 cardiomyocytes were measured randomly in each field and the average value was included in the

statistics. h. The relative mRNA expression of β-MHC, calculated against GAPDH. i. Quantitative analysis of TUNEL. The cell nucleus was stained by TUNEL as positive, and the apoptosis rate was determined by the ratio of the positive cells and the total cell number. j-n. Expression levels and quantitative analysis of apoptotic (Caspase3, Bax) and anti-apoptotic (Bcl-2) proteins. The expression of GAPDH was used as the control. Value are mean ± SEM, n=8-10. #p<0.05 vs normal; * p<0.05 vs T2DM;

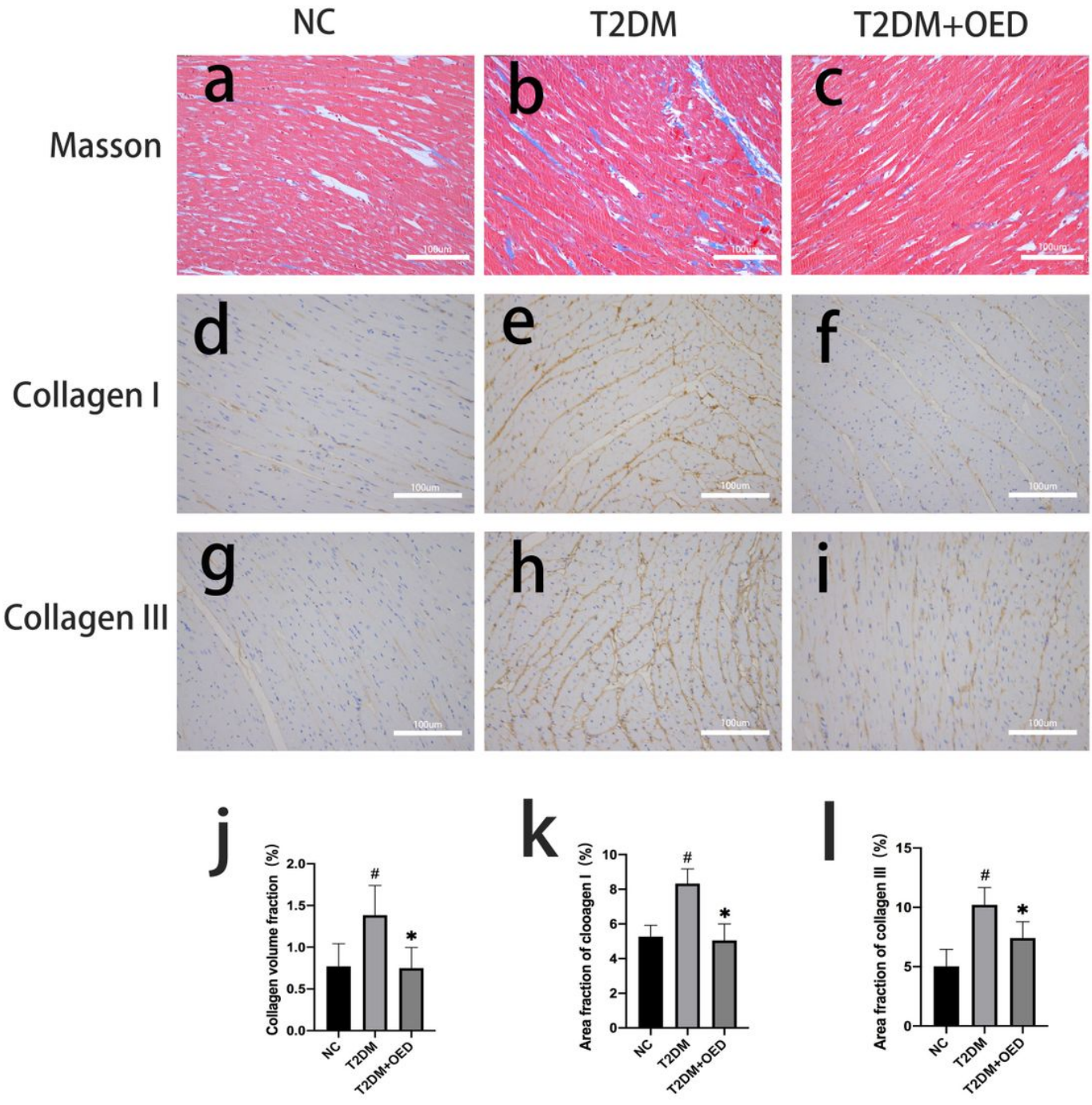


## Figure 3

OED attenuated diabetic myocardial fibrosis. (a-c). Masson's staining of myocardium (magnification x200, scale bar 100um). (d-i). Immunohistochemistry of collagen I and III (magnification x200, scale bar

100um). Each sample was taken three views for statistic. (j-l). Data are expressed as the mean ± SEM, n=8-10. #p<0.05 vs normal; * p<0.05 vs T2DM;

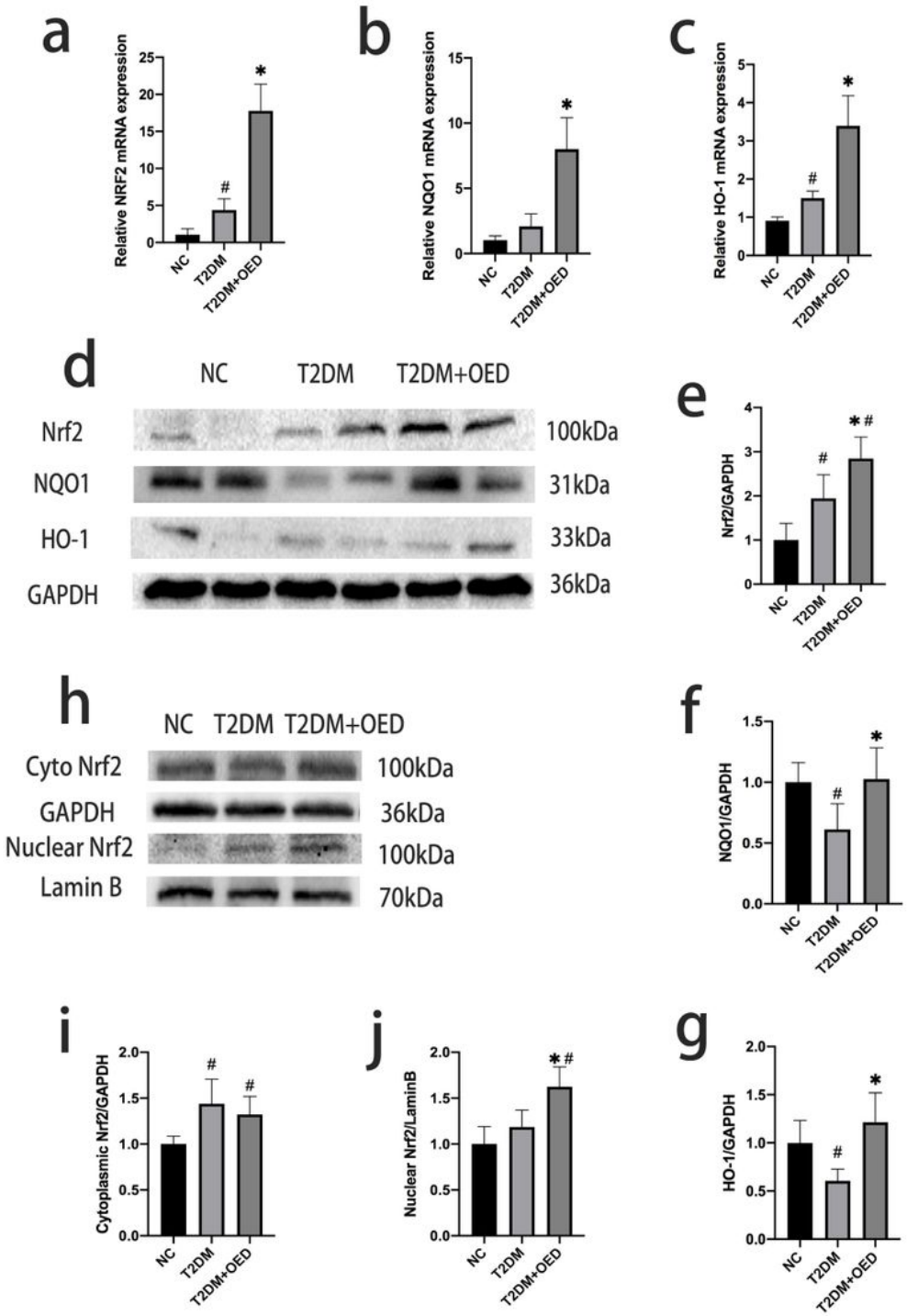


## Figure 4

OED activated Nrf2 pathway in diabetic rats. (a-c) The mRNA expression levels of Nrf2, HO-1 and NQO1 were evaluated by quantitative real-time polymerase chain reaction analysis, calculated against GAPDH. (d) The protein expression levels of Nrf2, HO-1 and NQO1 were evaluated by western blotting. (e-g)

Quantitative analysis of protein expression levels of Nrf2, HO-1 and NQO1. (h) The protein expression levels of nuclear and cytoplasmic Nrf2 were evaluated by western blotting. (i-j) Quantitative analysis of protein expression levels of nuclear and cytoplasmic Nrf2. The protein expression of GAPDH was used as the control of total and cytoplasmic protein and Lamin B as the nuclear protein. #p<0.05 vs normal; * p<0.05 vs T2DM;

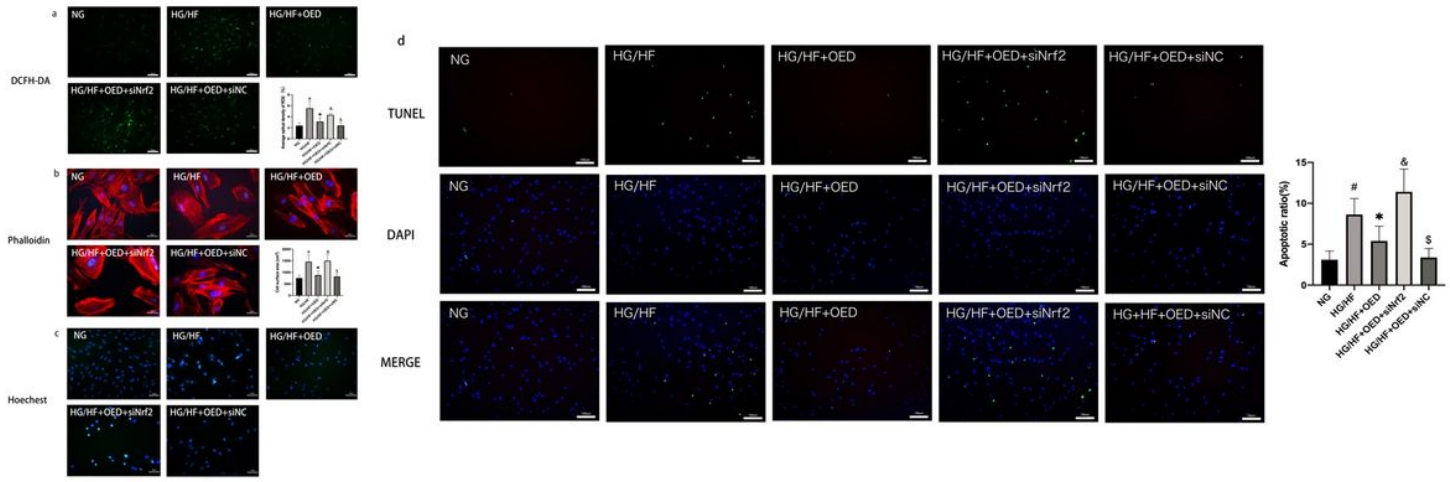


## Figure 5

The effects of OED attenuating HG/HF-Induced cardiomyocyte hypertrophy, reactive oxygen species and apoptosis could be canceled by silencing Nrf2. (a) Images and analysis of ROS detected by DCFH-DA. (magnification x100, scale bar 100um) (b) Images and analysis of cell surface area by F-actin stained with fluorescent phalloidin and DAPI counterstained nuclei. (magnification x400, scale bar 20um) (c) Images of apoptotic nuclei presented by Hoechst33342. (magnification x200, scale bar 50um). (d) Images and analysis of apoptotic nuclei detected by TUNEL. (magnification x100, scale bar 100um). Three views were taken randomly from each coverslip for calculation. Data are mean ± SEM of three independent experiments.

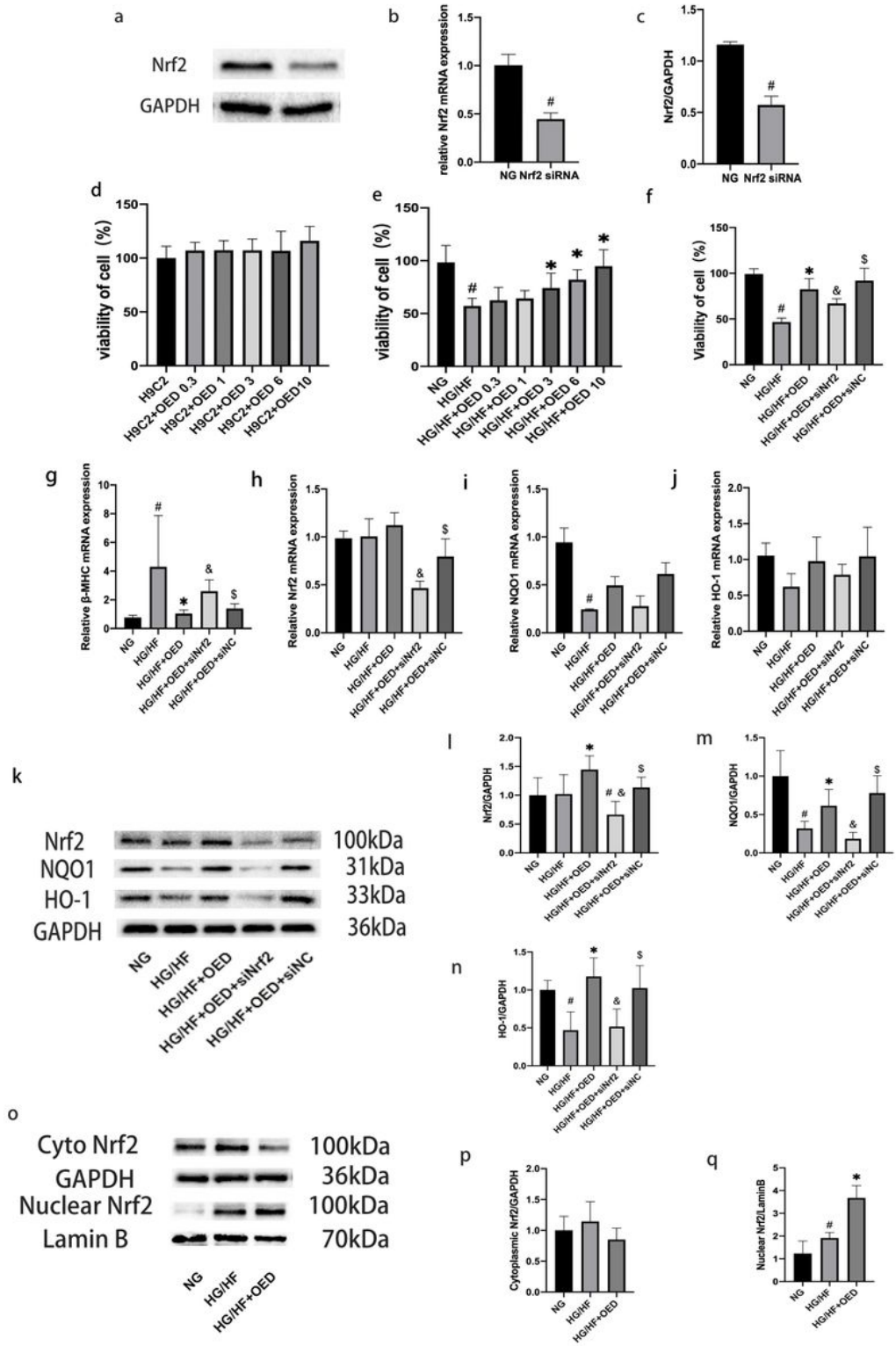


## Figure 6

OED attenuated H9C2 cardiomocytes injured by HG/HF via Nrf2 pathway. (a-c) Effect of Nrf2 siRNA transfection in H9C2, which detected by RT-qPCR and western blotting; (d) Viability of H9C2 cells after incubated with OED at different concentrations (ug/l) for 48h; (e) Effect of OED at different concentrations on HG/HF-induced damage in H9C2 cells. (f) Effect of OED on HG/HF-induced damage in H9C2 cells with or without siNrf2 transfection. (g-j) The mRNA expression levels of β-MHC, Nrf2,

NQO1and HO-1 were evaluated by quantitative real-time polymerase chain reaction analysis, calculated against GAPDH. (k) The protein expression levels of Nrf2, HO-1 and NQO1 were evaluated by western blotting. (l-n) Quantitative analysis for the protein levels of Nrf2, NQO1 and HO-1. (o) The protein expression levels of nuclear and cytoplasmic Nrf2 were evaluated by western blotting. (p, q) Quantitative analysis for the protein levels of nuclear and cytoplasmic Nrf2. The protein expression of GAPDH was used as the control of total and cytoplasmic protein and Lamin B as the nuclear protein. #$p<0.05$ vs normal; * $p<0.05$ vs T2DM;